

ORIGINAL RESEARCH

Dissecting the Imbalance of Synovial Macrophages in Rheumatoid Arthritis

Qing Li, MD; Wenping Liu, MD; Jibo Wang, PhD

ABSTRACT

Objective • This study sought to identify candidate genes of rheumatoid arthritis (RA) synovial macrophages using bioinformatics and to explore their pathways in the pathogenesis of RA.

Methods • The microarray datasets GSE10500 and GSE97779 were obtained from the Gene Express Omnibus and analyzed with synovial macrophages of 14 RA patients and 8 healthy donors. The researchers used R software to identify differentially expressed genes and determine functional enrichment pathways. A protein–protein interaction network was then constructed using STRING and Cytoscape. Gene expression was validated with the GSE71370 dataset and RT–qPCR analysis.

Results • 102 DEGs were identified in RA synovial macrophages relative to normal samples. Of these, 72 were

upregulated; 30 were downregulated. GO and KEGG pathway analyses suggested that DEGs mainly regulated the immune response and signaling pathways associated with inflammatory activation, apoptosis, and cancer. The top five hub genes and top 1 gene module from the PPI network of DEGs were *VEGFA*, *MMP9*, *FN1*, *IGF1*, *CXCL9*, *ISG20*, *RSAD2*, *IFI27*, *GBP2*, and *GBP1*. The GSE71370 dataset and RT–qPCR analysis showed that *CXCL9* and *GBP1* were significantly upregulated ($P \leq .05$).

Conclusions • *CXCL9* and *GBP1* may contribute to RA pathogenesis and serve as potential biomarkers and therapeutic targets for RA. (*Altern Ther Health Med*. 2023;29(7):434-439).

Qing Li, MD, Resident doctor; **Wenping Liu, MD**, Resident doctor; **Jibo Wang, PhD**, Chief physician; Department of Rheumatoid and Clinical Immunology, Affiliated Hospital of Qingdao University, Qingdao, China.

Corresponding author: Jibo Wang, PhD
E-mail: wangjibo2005@126.com

INTRODUCTION

Rheumatoid arthritis (RA), one of the most common chronic, systemic, autoimmune diseases, is characterized by joint synovitis and is estimated to affect approximately 1% of the adult population (ages 18 and older) worldwide.¹ Typically, synovial hyperplasia and inflammatory mononuclear cell infiltration result in joint inflammation and dysfunction, the hallmark of RA underlying several pathological processes.² Of note, systemic complications of RA, including cardiovascular diseases, interstitial lung diseases, and malignancies, lead to significantly increased mortality.^{3,4}

The pathogenesis associated with RA has been ascribed to an activated inflammatory response of synovium tissue and increased circulating monocytes migrated from peripheral

blood into the joints. During this process, remarkably, macrophages are another cell type widely recruited in RA synovial tissue, where they produce several pro-inflammatory cytokines such as tumor necrosis factor- α (TNF- α) and interleukin-1 β (IL-1 β), promoting synovial fibroblast proliferation, synovial hyperplasia, cartilage destruction, and bone lesions of RA joints.⁵⁻⁷ Consequently, stimulated synovial macrophages secrete high levels of chemokines CXCL1 that reinforce monocyte and neutrophil influx, leading to sustained inflammation.⁸ While macrophages appear to play a central role in RA, little is known about the regulatory mechanisms driving RA-associated synovial tissue macrophages, underscoring a need for a better understanding of the molecular basis of RA pathogenesis. The present study seeks to identify the core factors leading to the imbalance of macrophages that results in RA progression.

By analyzing the gene expression of RA synovial macrophages followed by RT-PCR validation, the researchers identified the top five hub genes and the leading gene module from the PPI network of differentially expressed genes (DEGs). Of these genes, *CXCL9* and *GBP1* were significantly greater in synovial macrophages of RA patients than in healthy individuals.

MATERIALS AND METHODS

Microarray data resources

The researcher obtained two datasets of RA synovial macrophages from the Gene Expression Omnibus (GEO). dataset GSE10500 was established with platform GPL8300 and contained data from synovial macrophage samples from five RA patients and three healthy individuals. Dataset GSE97779 was generated using platform GPL570 and involved data from synovial macrophages of nine RA patients and five healthy donors. Dataset GSE71370, based on platform GPL16268 was used as a validation set and contained data from peripheral blood macrophages of nine RA patients and eight healthy donors and synovial macrophages of nine RA patients.

Data preprocessing and identification of DEGs

The researchers employed R software (3.6.2) for data processing and statistical analyses. Data preprocessing involved background adjustment, normalization, and summarization. The Limma package served to identify DEGs in RA vs. normal synovial macrophages. Adjusted $P \leq .05$ and \log_2 -fold change (FC) ≥ 2 constituted the cut-off thresholds. DEGs co-expressed in two gene expression datasets using a Venn diagram.

GO and KEGG pathway analyses

Functional and pathway enrichment analyses of candidate DEGs used the clusterProfiler package. Visualization of the results used the GOplot package in R. False discovery rate (FDR) ≤ 0.05 and gene count > 2 were chosen as the cut-off thresholds.

PPI network analysis

STRING analysis generated the functional protein association networks for the DEGs. Interaction scores > 0.40 (medium confidence) were considered significant. Protein-protein interaction (PPI) networks were constructed using Cytoscape (3.7.2) and were analyzed using the MCODE plug-in module to identify densely connected regions with default parameters: degree cutoff ≥ 2 , node score cutoff ≥ 0.2 , K-core ≥ 2 , and max depth = 100. Functional annotation of DEGs in modules was analyzed using STRING with FDR ≤ 0.05 as the cut-off point.

Cell culture

An RPMI-1640 culture medium at 37°C and 5% CO₂ maintained the THP-1 cells. THP-1 cells were differentiated into macrophage-like cells (pTHP-1) by treating them with 10 ng/mL PMA for 48 h. Next, pTHP-1 cells were treated with 500 ng/mL LPS (Sigma, Cat No. L2630, St. Louis, MO, USA) for 24 h.

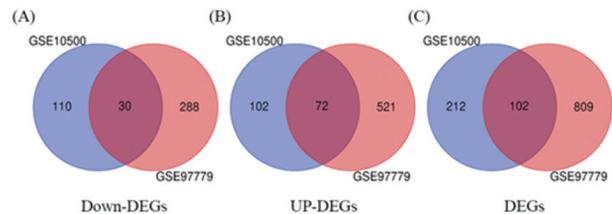
RT-qPCR

Total RNA was isolated using TRIzol (TaKaRa, Cat No. 9109, Tokyo, Japan) and dissolved in water. 1 µg of total RNA

Table 1. RT-qPCR primer sequences

Gene	Forward primer	Reverse primer
GAPDH	AACAGCCTCAAGATCATCAGCAA	GACTGTGGTCATGAGTCCTTCCA
VEGFA	AGGGCAGAATCATCACGAAGT	AGGGTCTCGATTGGATGGCA
MMP9	AGACCTGGGCAGATTCCAAAC	CGGCAAGTCTTCCGAGTAGT
FN1	CGGTGGCTGTCAAGTCAAAG	AAACCTCGGCTTCTCCATAA
IGF1	GCTCTTCAGTTCGTGTGTGGA	GCCTCCTTAGATCACAGCTCC
CXCL9	ATCTTGCTGGTTCTGATTGGAGTG	AAGGTCTTTCAAGGATTGTAGGTG
GBP1	AGGAGTTCCTTCAAAGATGTGGA	GCAACTGGACCCTGTCGTT
GBP2	CATCCGAAAGTTCTTCCCCAA	CTCTAGGTGAGCAAGGTACTTCT
RSAD2	CAGCGTCAACTATCACTTCACT	AACTCTACTTTGCAGAACCTCAC
ISG20	CTCGTTGCAGCCTCGTGAA	CGGGTTCTGTAATCGGTGATCTC
IFI27	TGCTCTCACCTCATCAGCAGT	CACAACCTCTCCAATCAAACT

Figure 1. Venn diagrams of DEGs. (A) Down-DEGs in the two datasets. (B) Up-DEGs in the two datasets. (C) DEGs in the two datasets.



was reverse transcribed using random hexamers and PrimeScript RT Reagent Kit. (TaKaRa, Cat No. RR037A, Tokyo, Japan) A SYBR Green Mastermix kit (TaKaRa, Cat No. RR820A, Tokyo, Japan) processed the resulting cDNA for reactions. The 2- $\Delta\Delta C_t$ method determined the relative gene expression scale to GAPDH. GraphPad Prism 8 (GraphPad Prism, La Jolla, CA, USA) analyzed the data to find that $P \leq .05$ indicates statistical significance. Table 1 lists the gene-specific primers used in the RT-PCR analyses.

RESULTS

Identification of DEGs

The researchers standardized GSE10500 and GSE97779 datasets using the KNN algorithm to identify and replace the missing values with numeric ones. A Venn diagram of the relationship between DEG groups showed that, from a total of 14 RA and 8 normal control samples, 102 DEGs were identified, of which 72 were upregulated and 30 were downregulated (Figure 1).

Enrichment analysis

To determine the critical biological functions and key signaling pathways of these DEGs, GO analysis and KEGG pathway analysis were performed using the clusterProfiler package. R. GO analysis showed that the 102 DEGs identified via the KNN algorithm were mainly associated with the regulation of immune system processes (such as antimicrobial humoral response, defense response to a virus, responses to a virus and an antibiotic) in Biological Process (BP), external side of plasma membranes (such as secretory granule lumen and cytoplasmic vesicle lumen) in Cell Component (CC), and antigen-binding (such as glycosaminoglycan binding,

Table 2. GO enrichment terms of DEGs

ONTOLOGY	ID	Description	P value	Gene Count
BP	GO:0019730	antimicrobial humoral response	.0048	7
	GO:0051607	defense response to virus	.0048	9
	GO:0009615	response to virus	.0048	10
	GO:0046677	response to antibiotic	.0048	10
	GO:0032496	response to lipopolysaccharide	.0048	10
	GO:0050900	leukocyte migration	.0048	12
	GO:0002237	response to molecule of bacterial origin	.0048	10
	GO:0034113	heterotypic cell-cell adhesion	.0053	5
	GO:0045861	negative regulation of proteolysis	.0061	10
CC	GO:0052547	regulation of peptidase activity	.0066	11
	GO:0034774	secretory granule lumen	.0006	10
	GO:0060205	cytoplasmic vesicle lumen	.0006	10
	GO:0031983	vesicle lumen	.0006	10
	GO:0031093	platelet alpha granule lumen	.0012	5
	GO:0031091	platelet alpha granule	.0042	5
	GO:0009897	external side of plasma membrane	.0311	8
MF	GO:0070820	tertiary granule	.0446	5
	GO:0005775	vacuolar lumen	.0481	5
	GO:0005539	glycosaminoglycan binding	.0390	7
	GO:0042379	chemokine receptor binding	.0390	4
	GO:0019955	cytokine binding	.0390	5
	GO:0033218	amide binding	.0390	8
	GO:0048029	monosaccharide binding	.0390	4
	GO:0070851	growth factor receptor binding	.0390	5
	GO:0001540	amyloid-beta binding	.0390	4
	GO:0005126	cytokine receptor binding	.0390	7
	GO:0015144	carbohydrate transmembrane transporter activity	.0390	3
	GO:0042277	peptide binding	.0390	7

Figure 2. Enrichment analyses of DEGs. (A) The top 10 GO enrichment terms in each group. The Y-axis represents GO terms. The X-axis represents number of enriched genes. The gradual color scale represents the *p* adjust-value. (B) The top-20 KEGG pathways. The X-axis represents the gene ratio, indicating the gene number. The Y-axis represents signaling pathways. Dot size represents gene number. The gradual color scale represents correlation.

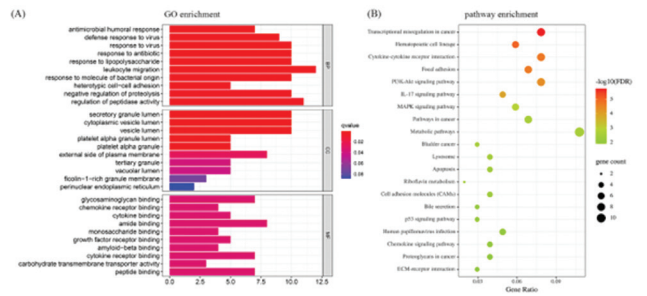
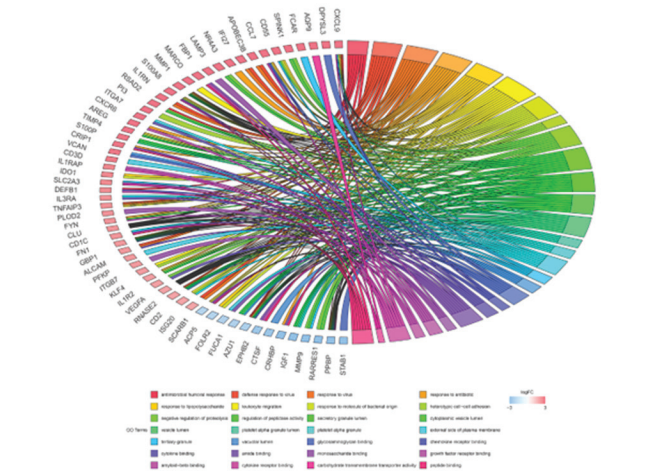


Figure 3. Circos plot of the relationships between genes and GO terms. The gradual color of the outer circle genes represents log FC, red shapes represent up-DEGs, blue shapes represent down-DEGs.



chemokine receptor binding and cytokine binding) in Molecular Function (MF). Table 2 and Figures 2-3 illustrated the top 10 terms in the 3 groups. Intriguingly, the top 20 enriched KEGG biological pathways were primarily enriched in transcriptional mis-regulation in cancer, hematopoietic cell lineage, cytokine-cytokine receptor interaction, focal adhesion, PI3K-Akt signaling pathway, and IL-17 signaling pathway (Table 3 and Figure 3).

PPI network and module analysis

To further establish a PPI network between RA and normal samples, the researchers identified 195 interactions and 83 nodes, including 61 upregulated and 22 downregulated DEGs via STRING and Cytoscape, and revealed the top 5 hub genes with the highest scores: *VEGFA*, *MMP9*, *FN1*, *IGF1*, and *CXCL9* (Figure 4). In addition, the Cytoscape MCODE plugin (Table 4) identified 5 PPI network modules.

Table 3. The top 20 KEGG pathway enrichment terms of DEGs

ID	Pathway name	gene count	FDR
hsa05202	Transcriptional misregulation in cancer	8	1.77E-06
hsa04640	Hematopoietic cell lineage	6	1.02E-05
hsa04060	Cytokine-cytokine receptor interaction	8	1.97E-05
hsa04510	Focal adhesion	7	2.09E-05
hsa04151	PI3K-Akt signaling pathway	8	4.69E-05
hsa04657	IL-17 signaling pathway	5	1.18E-04
hsa04010	MAPK signaling pathway	6	1.24E-03
hsa05200	Pathways in cancer	7	2.80E-03
hsa01100	Metabolic pathways	11	2.96E-03
hsa05219	Bladder cancer	3	3.06E-03
hsa04142	Lysosome	4	3.60E-03
hsa04210	Apoptosis	4	4.70E-03
hsa00740	Riboflavin metabolism	2	5.03E-03
hsa04514	Cell adhesion molecules (CAMs)	4	5.40E-03
hsa04976	Bile secretion	3	8.71E-03
hsa04115	p53 signaling pathway	3	8.71E-03
hsa05165	Human papillomavirus infection	5	8.89E-03
hsa04062	Chemokine signaling pathway	4	1.00E-02
hsa05205	Proteoglycans in cancer	4	1.20E-02
hsa04512	ECM-receptor interaction	3	1.22E-02

Figure 4. (A) PPI network of DEGs. Red shapes represent up-DEGs. Blue shapes represent down-DEGs. The gradual color scale represents the log FC. Node size represents degree value. (B) Degree scores of the top-30 hub genes.

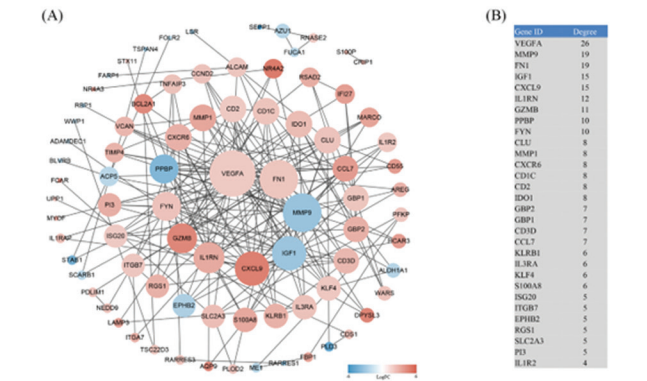


Figure 5. Top 2 cluster modules from the PPI network. Red octagons represent up-DEGs. Blue octagons represent down-DEGs. (A) Module one, (B) KEGG enrichment pathways of module one, (C) module two, and (D) KEGG enrichment pathways of module two.

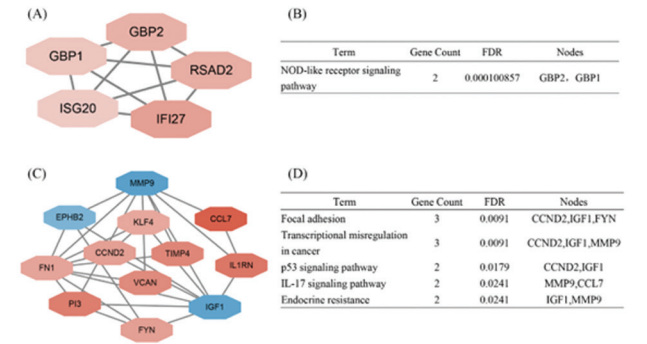


Table 4. PPI network modules of DEGs in RA

Cluster	Score	Nodes	Edges	Node IDs
1	5	5	10	ISG20, RSAD2, IFI27, GBP2, GBP1
2	4.727	12	26	FN1, EPHB2, MMP9, TIMP4, IGF1, CCL7, VCAN, PI3, CCND2, FYN, IL1RN, KLF4
3	3	3	3	CD2, CD1C, GZMB
4	3	3	3	ME1, PFKF, FBP1
5	3	3	3	AZU1, RNASE2, FUCA1

Figure 6. Verification of the key genes by the GSE71370 dataset. (A) Expression levels of the top 5 hub genes. (B) Expression levels of genes in the top 1 gene module. * $P < .05$, ** $P < .01$, *** $P < .0001$.

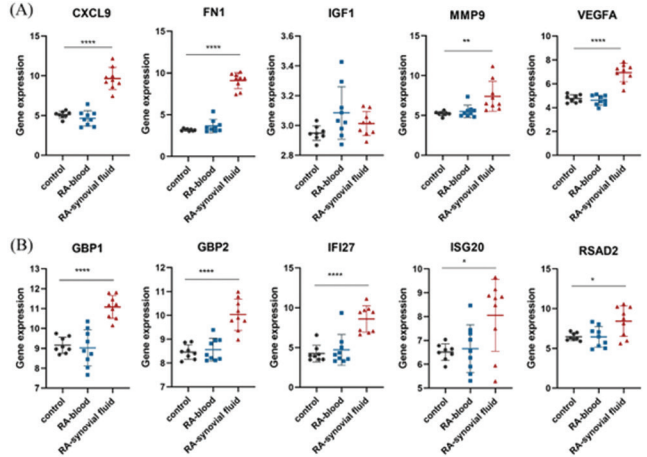
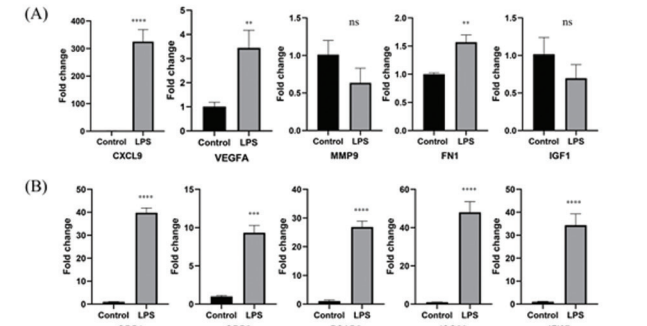


Figure 7. RT-qPCR analysis of key gene expression in macrophages vs. control cells. (A) Expression levels of the top 5 hub genes. (B) Expression levels of genes in the top 1 gene module. * $P < .05$, ** $P < .01$, *** $P < .0001$, ns, non-significant.



Of these top 2 significant modules were shown to be associated with NOD-like receptor signaling, focal adhesion, transcriptional mis-regulation in cancer, and the p53 signaling pathway, revealed by KEGG analyses (Figure 5).

Validation of the key genes

To validate these in silico analysis suggested data, we evaluated the expressions of the top 5 hub genes and the top gene module by another dataset (GEO accession: GSE71370) and followed by RT-qPCR analysis. Compared to normal samples, the gene expression levels of *CXCL9*, *VEGFA*, *FN1*,

ISG20, *RSAD2*, *IFI27*, *GBP2*, and *GBP1* had significantly elevated RA synovial macrophages and inflammatory macrophages ($P \leq .05$, Figures 6-7), in consistence with our bioinformatics analysis above.

DISCUSSION

Rheumatoid arthritis is a systemic autoimmune disorder characterized by synovial joint inflammation. Macrophages are resident cells in synovial tissue and can orchestrate cytokine-driven inflammation in RA, leading to persistent synovial inflammation and associated bone damage.⁹ Several lines of evidence showed that macrophages play a pivotal role in RA onset and progression. However, fundamental gaps remain in our understanding of the imbalance of synovial macrophages during RA development. Here, using numerous bioinformatic analyses, including the KNN algorithm, GO and KEGG pathway analyses, STRING and Cytoscape, and the Cytoscape MCODE plugin, the researchers identified key genes and pathways associated with RA synovial macrophages to serve as biomarkers and therapeutic targets for RA.

With recent advancements in transcriptome analysis, several groups reported the gene expression data of synovial macrophages in RA patients to dissect the underlying molecular mechanism. The researchers standardized the data from two independent datasets to obtain more reliable results and validated the results with a third. The 102 DEGs identified were primarily associated with regulating immune response and signaling pathways closely linked to inflammatory activation, apoptosis, and cancer. Of these, *CXCL9*, *VEGFA*, *FN1*, *ISG20*, *RSAD2*, *IFI27*, *GBP2*, and *GBP1* were markedly elevated in synovial macrophages of RA relative to what of healthy donors and peripheral blood macrophages from RA patients.

Consistent with previous findings,¹⁰ the present study found *CXCL9* as the top upregulated gene in RA synovial macrophages and involved in all of the top 7 biological processes in the GO functional enrichment analysis. *CXCL9* is an interferon- γ (IFN- γ)-inducible chemokine that promotes lymphocyte migration to RA synovial tissues by binding to its receptor *CXCR3*.^{11,12} The interaction between *CXCL9* and *CXCR3* may stimulate Src phosphorylation,¹³ a possible mechanism involved in the activation of PI3K-Akt signaling in RA synovial macrophages. Of interest, the antigen-induced arthritic mice model emphasized that *CXCL9*-derived peptides diminished neutrophil recruitment and joint inflammation by interfering with glycosaminoglycan interactions,¹⁴ highlighting *CXCL9* as a potential therapeutic target for RA. Many groups have proposed various chemokine receptors as therapeutic targets for RA, including *CCR7*, *CX3CL1*, *CXCR4*, and *CCR9*.¹⁵⁻¹⁸ Given that *CXCL9* was the only chemokine to emerge from the present analysis, it would be interesting if future studies explored possible understandings how *CXCL9*-*CXCR3* pairs trigger the RA onset and progression. It would also be worthwhile to evaluate whether targeting a *CXCL9*-*CXCR3* interaction would benefit from the development of a promising new therapeutic modality.

This study provided the first evidence that GBP, especially *GBP1*, is implicated in an imbalance of synovial macrophages during RA development. *GBP1* and *GBP2* belong to the interferon-inducible GTPases family that promote antimicrobial immunity and mediate inflammation and cell cycle progression.¹⁹ *GBP1* and *GBP2* are the most highly expressed interferon-stimulated genes (ISGs) in humans²⁰. More recent data hint at interferon-stimulated gene involvement in RA. *GBP1* is highly expressed in the serum and synovial tissues of RA patients.²¹ Moreover, in infected macrophages, *GBP1* enhances gasdermin-D-dependent macrophage apoptosis and pyroptosis due to the recruitment and activation of caspase-4.²² This study's KEGG enrichment analysis indicated that *GBP1* and *GBP2* participated in NOD-like receptor signaling, another mechanism by which macrophage lose the balance in RA. Intriguingly, several other identified gene products, such as *ISG20*, *RSAD2*, and *IFI27*, also listed in the top gene module, are ISGs and were reported to connect to RA,²³⁻²⁵ highlighting the pivotal role of interferon in RA.

CONCLUSIONS

This study identified *CXCL9* and *GBP1* as candidate genes for RA synovial macrophages in RA pathogenesis. These findings advance the understanding of RA pathogenesis and pave the way for developing innovative diagnostic strategies and identifying new therapeutic targets for RA.

DATA AVAILABILITY

The RNA-seq data that support the findings of this study are available in the GEO database (<https://www.ncbi.nlm.nih.gov/geo/>) with the following data accession identifiers: GSE10500, GSE97779, and GSE71370.

CONFLICTS OF INTEREST

The authors declare that they have no competing interests.

ACKNOWLEDGMENTS

The authors thank all the members of our research group for their enthusiastic participation.

REFERENCES

- Scott DL, Wolfe F, Huizinga TW. Rheumatoid arthritis. *Lancet*. 2010;376(9746):1094-1108. doi:10.1016/S0140-6736(10)60826-4
- Catrina AI, Joshua V, Klareskog L, Malmström V. Mechanisms involved in triggering rheumatoid arthritis. *Immunol Rev*. 2016;269(1):162-174. doi:10.1111/imr.12379
- Hylgaard C, Hilberg O, Pedersen AB, et al. A population-based cohort study of rheumatoid arthritis-associated interstitial lung disease: comorbidity and mortality. *Ann Rheum Dis*. 2017;76(10):1700-1706. doi:10.1136/annrheumdis-2017-211138
- Figus FA, Piga M, Azzolin I, McConnell R, Iagnocco A. Rheumatoid arthritis: extra-articular manifestations and comorbidities. *Autoimmun Rev*. 2021;20(4):102776. doi:10.1016/j.autrev.2021.102776
- Chen Z, Bozec A, Rammig A, Schett G. Anti-inflammatory and immune-regulatory cytokines in rheumatoid arthritis. *Nat Rev Rheumatol*. 2019;15(1):9-17. doi:10.1038/s41584-018-0109-2
- Kondo N, Kuroda T, Kobayashi D. Cytokine Networks in the pathogenesis of rheumatoid arthritis. *Int J Mol Sci*. 2021;10(22):20922. doi:10.3390/ijms222010922
- McInnes IB, Schett G. Cytokines in the pathogenesis of rheumatoid arthritis. *Nat Rev Immunol*. 2007;7(6):429-442. doi:10.1038/nri2094
- Ji RR, Chamesian A, Zhang YQ. Pain regulation by non-neuronal cells and inflammation. *Science*. 2016;354(6312):572-577. doi:10.1126/science.aaf8924
- Siouti E, Andreaskos E. The many facets of macrophages in rheumatoid arthritis. *Biochem Pharmacol*. 2019;165:152-169. doi:10.1016/j.bcp.2019.03.029
- Yoshida S, Arakawa F, Higuchi F, et al. Gene expression analysis of rheumatoid arthritis synovial lining regions by cDNA microarray combined with laser microdissection: up-regulation of inflammation-associated STAT1, IRF1, CXCL9, CXCL10, and CCL5. *Scand J Rheumatol*. 2012;41(3):170-179. doi:10.3109/03009742.2011.623137
- Ruschpler P, Lorenz P, Eichler W, et al. High CXCR3 expression in synovial mast cells associated with CXCL9 and CXCL10 expression in inflammatory synovial tissues of patients with rheumatoid arthritis. *Arthritis Res Ther*. 2003;5(5):R241-R252. doi:10.1186/ar783
- Yu X, Song Z, Rao L, et al. Synergistic induction of CCL5, CXCL9 and CXCL10 by IFN- γ and NLRs ligands on human fibroblast-like synoviocytes-A potential immunopathological mechanism for joint inflammation in rheumatoid arthritis. *Int Immunopharmacol*. 2020;82:106356. doi:10.1016/j.intimp.2020.106356
- Zhang C, Li Z, Xu L, et al. CXCL9/10/11, a regulator of PD-L1 expression in gastric cancer. *BMC Cancer*. 2018;18(1):462. doi:10.1186/s12885-018-4384-8

14. Boff D, Crijns H, Janssens R, et al. The chemokine fragment CXCL9(74-103) diminishes neutrophil recruitment and joint inflammation in antigen-induced arthritis. *J Leukoc Biol*. 2018;104(2):413-422. doi:10.1002/JLB.3MA1217-502R
15. Jakobs BD, Spannagel L, Purvanov V, Uetz-von Allmen E, Matti C, Legler DF. Engineering of nanobodies recognizing the human chemokine receptor CCR7. *Int J Mol Sci*. 2019;20(10):2597. doi:10.3390/ijms20102597
16. Nanki T, Imai T, Kawai S. Fractalkine/CX3CL1 in rheumatoid arthritis. *Mod Rheumatol*. 2017;27(3):392-397. doi:10.1080/14397595.2016.1213481
17. Tamamura H, Fujisawa M, Hiramatsu K, et al. Identification of a CXCR4 antagonist, a T140 analog, as an anti-rheumatoid arthritis agent. *FEBS Lett*. 2004;569(1-3):99-104. doi:10.1016/j.febslet.2004.05.056
18. Yokoyama W, Kohsaka H, Kaneko K, et al. Abrogation of CC chemokine receptor 9 ameliorates collagen-induced arthritis of mice. *Arthritis Res Ther*. 2014;16(5):445. doi:10.1186/s13075-014-0445-9
19. Feng S, Man SM. Captain GBP1: inflammasomes assemble, pyroptotic endgame. *Nat Immunol*. 2020;21(8):829-830. doi:10.1038/s41590-020-0727-0
20. Schneider WM, Chevillotte MD, Rice CM. Interferon-stimulated genes: a complex web of host defenses. *Annu Rev Immunol*. 2014;32(1):513-545. doi:10.1146/annurev-immunol-032713-120231
21. Zhang F, Wei K, Slowikowski K, et al; Accelerating Medicines Partnership Rheumatoid Arthritis and Systemic Lupus Erythematosus (AMP RA/SLE) Consortium. Defining inflammatory cell states in rheumatoid arthritis joint synovial tissues by integrating single-cell transcriptomics and mass cytometry. *Nat Immunol*. 2019;20(7):928-942. doi:10.1038/s41590-019-0378-1
22. Fisch D, Bando H, Clough B, et al. Human GBP1 is a microbe-specific gatekeeper of macrophage apoptosis and pyroptosis. *EMBO J*. 2019;38(13):e100926. doi:10.15252/embj.2018100926
23. Zheng Z, Wang L, Pan J. Interferon-stimulated gene 20-kDa protein (ISG20) in infection and disease: review and outlook. *Intractable Rare Dis Res*. 2017;6(1):35-40. doi:10.5582/iridr.2017.01004
24. Castañeda-Delgado JE, Bastián-Hernandez Y, Macías-Segura N, et al. Type I interferon gene response is increased in early and established rheumatoid arthritis and correlates with autoantibody production. *Front Immunol*. 2017;8:285. doi:10.3389/fimmu.2017.00285
25. Wampler Muskardin TL, Fan W, Jin Z, et al. Distinct single cell gene expression in peripheral blood monocytes correlates with tumor necrosis factor inhibitor treatment response groups defined by type I interferon in rheumatoid arthritis. *Front Immunol*. 2020;11:1384. doi:10.3389/fimmu.2020.01384